Comparison of Au and Pt Foils for an Imaging Bolometer

Byron J. PETERSON, Evgeny A. DRAPIKO, Dongcheol SEO[1)] and Naoko ASHIKAWA

National Institute for Fusion Science, 322-6 Oroshi-cho, Toki 509-5292, Japan
[1)] *National Fusion Research Institute, Daejeon 305-806, Republic of Korea*

(Received 19 March 2010 / Accepted 16 July 2010)

In the imaging bolometer a thin metal foil converts plasma radiated power to infrared radiation measured by an infrared camera. Calibration of the foil provides information on its sensitivity, which is helpful in selecting the best foil material. In this study thermal properties of submicron Au and Pt foils are investigated by heating the foils with a chopped HeNe laser beam (~20 mW) and observing the temperature change, ΔT, and thermal time constant, τ, of the foil temperature. Assuming that the foil cooling is dominated by diffusion, we can compare the relative sensitivities of the foils by comparing the ratio of the thermal diffusivity to the thermal conductivity of the foil, κ/k, to the ratio $\Delta T/\tau$. The results indicate that Pt is more than 9 times more sensitive than Au even though standard thermal properties indicate that Au should be slightly (14%) more sensitive than Pt. This inconsistency indicates that the IR radiation is dominant over diffusion in the foil cooling. In that case the sensitivity should be evaluated by $1/k \sim \Delta T$, which indicates that Pt is 8 times more sensitive than Au, while the ratio of thermal conductivities indicates that it should be only 4 times more sensitive.

Keywords: bolometer, plasma diagnostics, infrared radiation, imaging diagnostics, calibration

DOI: 10.1585/pfr.5.035

1. Introduction

Bolometer diagnostics are essential for the measurement of radiated power loss from fusion devices [1]. The InfraRed imaging Video Bolometer (IRVB) has been under development for application to a fusion reactor due to its durability vis-à-vis neutrons and gammas and its lack of in-vessel wires and the numerous vacuum feedthroughs which plague conventional resistive bolometers [2–4]. Also it provides an image of the radiation from the plasma which can be useful for steady-state reactor operation [5].

An IRVB consists of a thin metal foil mounted in a copper frame which absorbs the radiation from the plasma through an aperture. Viewing the foil from the opposite side is an IR camera which is used to measure the change in the foil temperature due to the absorbed radiation. The radiation profile on the foil is obtained by solving the two-dimensional heat diffusion equation for the foil. In order to do so the thermal characteristics of the foil including the product of the thermal conductivity, k, and the foil thickness, t_f, the thermal diffusivity, κ, and the blackbody emissivity, ε, must be determined. Since the foil is blackened with a graphite coating for good IR emissivity, and due to non-uniformity in the manufacturing of the foils, these properties can vary considerably across the foil and from the standard values found in reference handbooks [6]. Therefore it is important to measure these properties carefully to insure the calibration of the diagnostic and to evaluate which foil material is the most sensitive.

author's e-mail: peterson@LHD.nifs.ac.jp

The noise equivalent power density, S_IRVB, of the IRVB is given by the following equation [7]

$$S_\mathrm{IRVB} = \frac{\sqrt{2}kt_\mathrm{f}\sigma_\mathrm{IR}}{\sqrt{f_\mathrm{IR}N_\mathrm{IR}}}\sqrt{\frac{5N_\mathrm{bol}^3 f_\mathrm{bol}}{A_\mathrm{f}^2}+\frac{N_\mathrm{bol}f_\mathrm{bol}^3}{\kappa^2}} \qquad (1)$$

in terms of the IR camera parameters: sensitivity, σ_IR, frame rate, f_IR, and number of pixels, N_IR, the foil properties: area, A_f, thickness, t_f, thermal conductivity, k, and thermal diffusivity, κ, and the IRVB parameters: frame rate, f_bol and number of channels, N_bol. A bolometer channel is typically the average over tens of IR camera pixels, which reduces noise and increases sensitivity at the expense of the number of bolometer channels or spatial resolution. The blackbody radiation term is not included since it is negligible for background temperatures below 1000°K. In normal applications the term on the right side under the radical dominates, therefore we can write $S_\mathrm{IRVB} \propto kt_\mathrm{f}/\kappa$. This should be as small as possible for high sensitivity, therefore we can write the sensitivity of the IRVB in terms of the foil parameters as κ/kt_f.

Recently several candidate foil materials have been suggested for an IRVB. These include Au, Pt and Ta. Au is not a good choice for a reactor since it has a high neutron capture cross-section which has been observed to lead to transmutation to Hg [8]. Calibration work with Ta showed that its value of kt_f was two times larger than the standard values indicating a halving of its sensitivity [6]. In this paper we consider Pt for the first time and compare it to Au with which we have much experience. Pt is a good candidate for an imaging bolometer foil in that it has the highest

ability to stop photons among candidate materials (Pt, Au, W, Ta, Hf). With regard to application to a fusion reactor such as ITER it is also an excellent candidate in that it has the lowest neutron capture cross-section among candidate materials. One drawback of Pt is that it has a rather low tensile strength compared to W, Hf and Ta, which is on the same order as Au. However strength was not seen to be an issue for a thin Au foil in JT-60U, but stability may be an issue [6, 7], but this should be less of an issue on ITER where a 10 micron or thicker foil is needed. For a comparison of these parameters and the relative merits of each material see Table 2 in Ref. [7] and also Ref. [6]. The objective of this study is to determine which foil material (Au or Pt) would be most sensitive for future use on LHD and KSTAR, two large experiments without sizable amounts of neutrons and particularly for KSTAR which will initially employ a sub micron foil due to the low levels of input and radiated power anticipated in the early stages of the KSTAR project.

2. Experimental Technique

In order to evaluate the relative merits of gold and platinum foils we use a laser calibration technique to evaluate the sensitivity of the two foils. Foils with a nominal thickness of 2.5 microns are selected since the target is applications to LHD or KSTAR for which that thickness is sufficient to stop energetic photons. However when samples of the foil material were measured with a microbalance the average thicknesses were calculated to be 0.87 microns for the Pt foil and 0.63 microns for the Au foil. The foils are mounted in copper frames to expose an area of 7 cm × 9 cm then sprayed on both sides with graphite as shown in Fig. 1 and then mounted in a vacuum flange with a ZnSe IR window. Then the flange is mounted on a vacuum chamber as shown in Fig. 2. A chopped HeNe laser beam (~20 mW) is used to heat the foil at each of twenty positions on the foil starting in the center of the foil and moving step by step in 1 cm increments in both dimensions to cover one quadrant of the foil as shown in Fig. 3. A FLIR SC500 IR camera (microbolometer, 8 – 12 microns, 60 fps, 240 × 320 pixels with a close up lens) is used to measure the foil temperature. At each laser beam position the IR camera data is taken as a series of four 200 frame captures. The first is without the laser beam to provide a background image, the second is during the temperature rise after the laser beam shutter is opened, the third records the steady-state temperature profile due to the laser beam heating of the foil and the fourth records the decay of the foil temperature after the shutter is closed. The background temperature measurement is averaged over the 200 frames and subtracted from the remaining 600 frames. The steady state series is then averaged over the 200 frames and the peak, ΔT, of the temperature profile is found and measured. This quantity represents the spatial maximum of the temperature change due to the foil heating by the laser. The temperature rise and decay are fit to a modified Gaussian [4] to find the rise and decay time contstants, respectively, which are averaged to give an effective thermal time constant, τ, in order to partially remove the effect of the IR radiation. If we neglect the blackbody radiation from the foil then $\tau \propto 1/\kappa$ and $\Delta T \propto 1/kt_f$ and therefore the sensitivity can be written

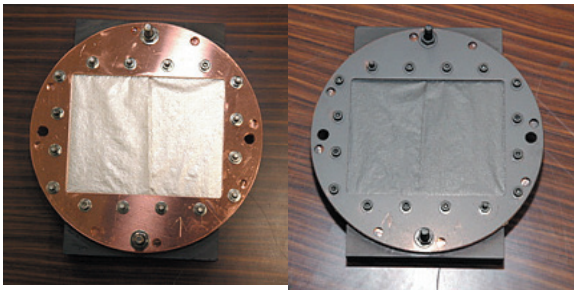

Fig. 1 Platinum foil mounted in copper frame before (left) and after (right) blackening with graphite.

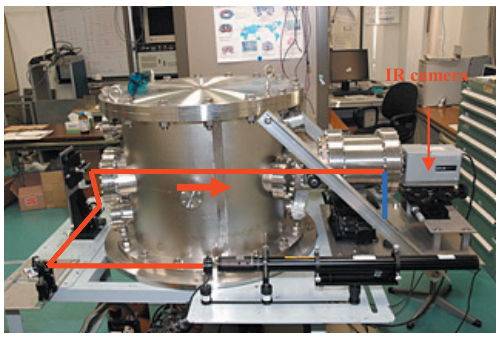

Fig. 2 Test stand showing laser path (red) and location of IRVB foil (blue line).

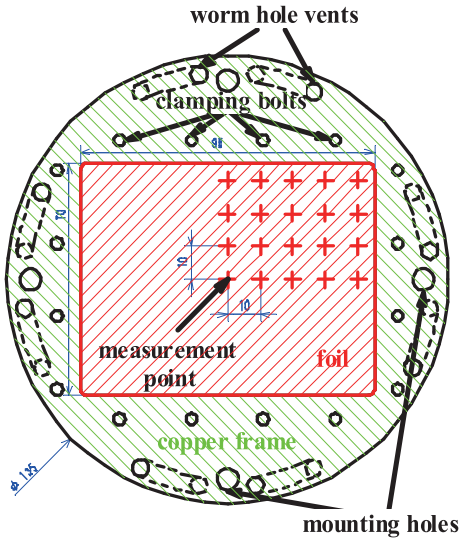

Fig. 3 Drawing of frame and foil showing location of 20 measurement points. Dimensions are shown in mm.

as

$$\kappa/k \propto \Delta T t_f/\tau S \quad (2)$$

where S is the laser beam power density. By comparing these parameters we can evaluate the relative sensitivity of the Au and Pt foils.

3. Results

The vertical and horizontal ΔT profiles when the laser beam is located at the center of the foil are shown in Fig. 4 for the Au and Pt foils. One notes that the temperature rise on the Pt foil is 32.7°C while that of the Au foil is 7.65°C or 5 times lower. When averaged over 20 points on the foil the average is 44.2°C for Pt and 7.15°C for Au giving a difference of a factor of 6. In Fig. 5 the foil temperature decays are shown for the peak ΔT position with the central laser position for the Pt and Au foils. The decays are fit to a modified Gaussian as shown in the figure giving decay times of 0.341 s (Pt) and 0.368 s (Au). Not shown are the temperature rise data when the shutter is opened which when fit to the modified Gaussian give rise times of 0.367 s (Pt) and 0.459 s (Au).

The spatial variations of the temperature rise and thermal time constants are shown in Figs. 6 and 7, respectively. These figures are made be combining the results from the point by point measurements to show the variations of those parameters across the foil. In terms of the peak temperature, the Au foil is relatively uniform varying from a high of 8.1°C to 6.3°C tending to decrease towards the edge as seen in Fig. 6 (a), while the Pt foil is less uniform with a minimum at the center of 32.7°C and tending to increase towards the edge with a maximum of 53.8°C as seen in Fig. 6 (b). Regarding the thermal time constants, these vary on the Au foil from 0.41 s at the foil center to 0.26 s at the edge as seen in Fig. 7 (a), while the Pt foil is more uniform with a variation from 0.35 s at the center to 0.29 s at the edge as seen in Fig. 7 (b).

Some of the variation in the foil temperature change and to a lesser extent the thermal time constant, can be attributed to variation in the transmission of the laser beam through the vacuum window as the laser beam was moved to heat different parts of the foil. This variation was on the order of 10%, but was difficult to reproduce and therefore it could not be compensated for. In future calibration work this problem will be avoided by using a new vacuum chamber with two-dimensional motion of the foil and a fixed IR camera and laser beam, instead of the current set-up where the foil is fixed and the IR camera and laser beam are moved. This will avoid variations in the window

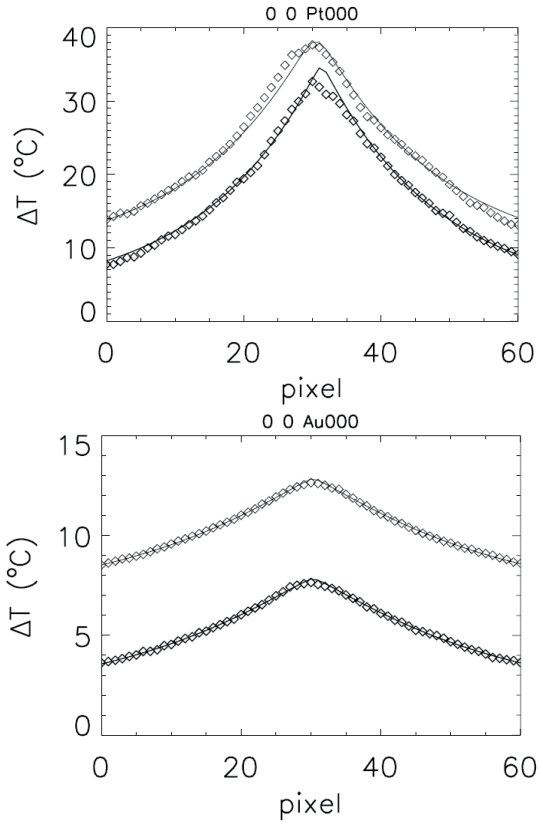

Fig. 4 Temperature profiles for Pt (upper) and Au (lower) foils are shown by symbols. In each plot the upper profile is the vertical profile and is offset by 5°C and the lower profile is the horizontal profile. Fits to a modified two-dimensional Gaussian are also shown by lines.

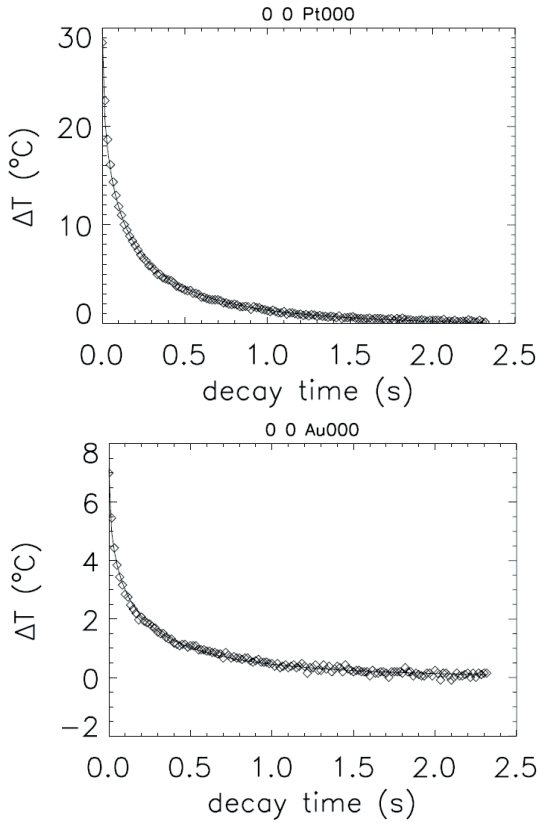

Fig. 5 Temperature decays (symbols) for Pt (upper) and Au (lower) foils and modified exponential fits (lines).

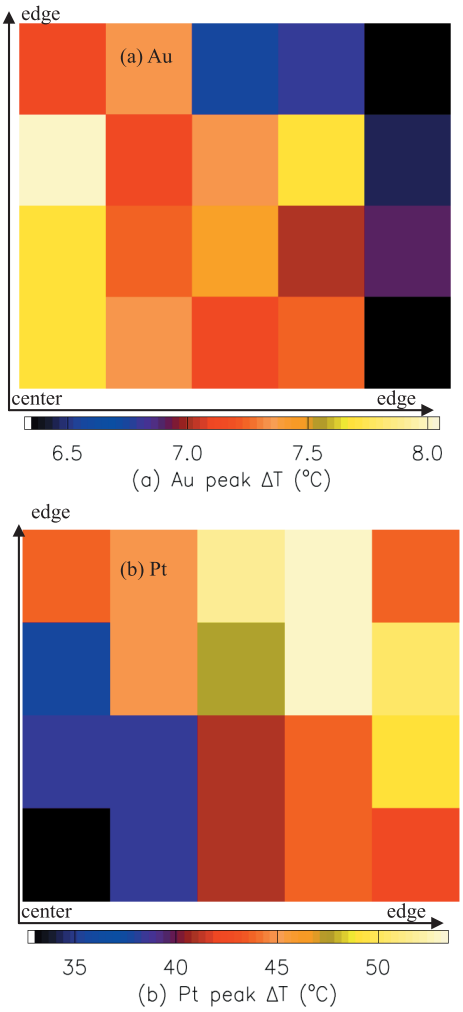

Fig. 6 Distribution of peak change in temperature on (a) gold and (b) platinum foils heated by a HeNe laser. The center pixel on the foil is in the lower left corner and the edges are on the upper and right sides.

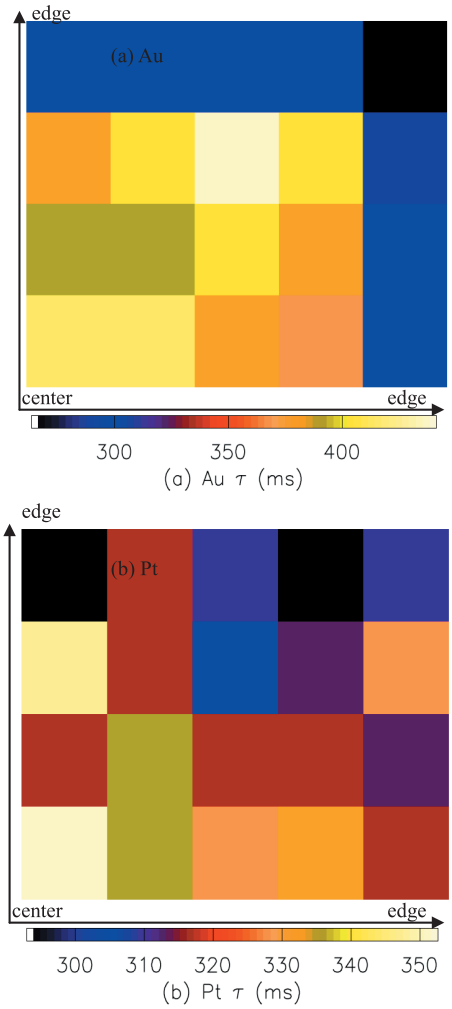

Fig. 7 Distribution of average thermal time constants on (a) gold and (b) platinum foils heated by a chopped HeNe laser beam. The center pixel on the foil is in the lower left corner and the edges are on the upper and right sides.

transmission of both the laser beam light and the infrared light and provide a more accurate calibration.

Taking the average of the rise and decay time constants for each point and averaging over the 20 points on the foil gives effective thermal time constants of 0.321 s (Pt) and 0.360 s (Au). If we combine τ, ΔT and slight variations in the laser beam power according to Eq. (2) then we get relative sensitivities of 5.4°C μm/smW (Pt) and 0.59°C μm/smW (Au). Therefore Pt is considered to be 9.2 times more sensitive than Au.

4. Discussion

Several observations deserve comment and discussion. First of all, regarding the steady state temperature rise, ΔT, we observed that this is 5 to 6 times higher for Pt than for Au. Since $\Delta T \propto 1/kt_f$, this may be partially explained by the difference in kt_f, which for the Au foil is 3.2 times greater than that of the Pt foil since Pt has a thermal conductivity which is 4.4 times smaller than that of Au.

Secondly, regarding the rise and decay time constants, we observe that the rise time constant is longer than the decay time constant. This is presumably due to the radiative cooling of the foil by infrared radiation. We attempt to mitigate the effect of this on our comparison of the two foil sensitivities by averaging the decay and rise time constants. Although this is not the correct way to compensate for this effect, it should remove it partially. In the same sense the temperature rise, ΔT, should also be affected by the infrared cooling. The higher the temperature rise the greater the cooling, therefore we estimate that the Pt data should be more strongly affected by the IR cooling, hence we expect that the actual difference between the two sensitivities should be even larger. Also regarding the thermal time constants, τ, we note that Pt has a slightly shorter thermal time constant than that of Au. However, for cooling of the foil dominated by diffusion $\tau \propto 1/\kappa$, we expect that the thermal time for Pt should be 5 times greater than that

for Au due to a five times smaller thermal diffusivity. This discrepancy, in addition to the previously described difference in the rise and decay time constants, indicates that blackbody (IR) radiation is more dominant than diffusion in the cooling of the foil. This would explain also why the Pt foil cools faster than the Au foil since its temperature is higher due to smaller k and therefore the IR cooling effect is greater. This would also explain why Pt is more than 9 times more sensitive than Au even though a comparison of the ratio of their thermal diffusivity to thermal conductivities would suggest that Au should be slightly more sensitive than Pt.

In addition, in terms of the spatial distributions of these quantities seen in Figs. 6 and 7, the gold foil shows a lower temperature change at the edge of the foil compared to the center, while the Pt foil has the opposite tendency. The average thermal time constants for Au are much lower near the edge while those for Pt are more uniform. Both of these trends confirm the earlier observation, based on a comparison of the relative values of the thermal time constants and temperature amplitudes, that the Pt foil is being cooled predominantly by radiation while the Au foil is being cooled by diffusion to the edge.

This indicates that our criteria for evaluating the sensitivity given by Eq. (2) may not be correct since this is based on the assumption that diffusion is dominating the cooling of the foil and the experimental evidence that we have is to the contrary (especially the difference between the rise and decay time constants). Therefore we should consider another criteria for the sensitivity, namely

$$1/k \propto \Delta T t_{\mathrm{f}}/P, \tag{3}$$

where P is the laser beam power. When this is considered the experimental values show that Pt is 8.1 times more sensitive that Au while the ratio of the thermal conductivities is 4.4. Therefore based on this criteria the Pt is still 8 times more sensitive than Au while the standard thermal parameters indicate that it should be only 4 times more sensitive.

We can conclude that Pt would be 8 or more times more sensitive than Au as long as the radiation dominates over the diffusion in the cooling of the foil. This is an important result for the initial stage of the KSTAR experiment when power levels will be small, or for smaller experiments in which power levels and photon energies are low, since a thinner foil would be adequate for those experiments. These results indicate that Pt is the best foil material choice for such experiments that can use a thin foil (less than 1 micron). We should confirm at which power levels the IR radiation dominates over the diffusion in the foil and make sure that the balance of these two cooling channels is properly handled in the solution of the heat diffusion equation for the incident radiated power. Also this effect should be checked in a thicker foil such as the 2.5 microns we plan to use eventually in KSTAR and LHD and the 10 microns that would be necessary for ITER.

This result indicates that we can raise the sensitivity of the IRVB by a factor of 8 or more by using Pt instead of Au. This should be an advantage for the IRVB compared to resistive bolometers since the resistive bolometer thermal time constant is determined by the diffusion through the insulating layer to the metal grid and not by blackbody radiation.

By raising the temperature of the foil and frame above that of the surrounding background we should be able to insure that the IR radiation term dominates over the diffusion and thereby reduce the diffusive term in the foil power balance equation. This will enable a more instantaneous measurement of the radiated power for real time imaging of the plasma radiation and will be tested in the near future.

Acknowledgement

This work was supported in part by a Grant-in-Aid for Science Research from the Japanese Ministry of Education, Culture, Sports, Science and Technology, 'Priority Area of Advanced Burning Plasma Diagnostics' (16082207) by NIFS Grant # ULPP-528 and by the Japan Korea Fusion Collaboration Program.

[1] A.W. Leonard *et al.*, Rev. Sci. Instrum. **66**, 1201 (1995).
[2] B.J. Peterson, Rev. Sci. Instrum. **71**, 3696 (2000).
[3] B.J. Peterson *et al.*, Rev. Sci. Instrum. **74**, 2040 (2003).
[4] H. Parchamy *et al.*, Rev. Sci. Instrum. **77**, 10E515 (2006).
[5] B.J. Peterson *et al.*, J. Nucl. Mater. **363-365**, 412 (2007).
[6] B.J. Peterson *et al.*, Rev. Sci. Instrum. **79**, 10E301 (2008).
[7] B.J. Peterson *et al.*, Plasma Fusion Res. **2**, S1018 (2007).
[8] T. Nishitani *et al.*, Fusion Eng. Des. **63-64**, 437 (2002).